Mathematical Biosciences and Engineering

http://www.aimspress.com/journal/mbe

MBE, 20(5): 9179–9207.
DOI: 10.3934/mbe.2023403
Received: 07 October 2022
Revised: 07 February 2023
Accepted: 11 February 2023
Published: 14 March 2023

Research article

How do classroom-turnover times depend on lecture-hall size?

Joseph Benson[1], Mariya Bessonov[2], Korana Burke[3], Simone Cassani[4], Maria-Veronica Ciocanel[5], Daniel B. Cooney[6] and Alexandria Volkening[7,*]

[1] Mathematics, Statistics, and Computer Science, Macalester College, Saint Paul, MN 55105, USA

[2] Department of Mathematics, NYC College of Technology, Brooklyn, NY 11201

[3] Department of Mathematics, University of California Davis, Davis, CA 95616

[4] Department of Mathematics, University at Buffalo, Buffalo, NY 14260

[5] Department of Mathematics and Department of Biology, Duke University, Durham, NC 27708

[6] Department of Mathematics and Center for Mathematical Biology, University of Pennsylvania, Philadelphia, PA 19104

[7] Department of Mathematics, Purdue University, West Lafayette, IN 47907

* **Correspondence:** Email: avolkening@purdue.edu; Tel: +17654961052.

Abstract: Academic spaces in colleges and universities span classrooms for 10 students to lecture halls that hold over 600 people. During the break between consecutive classes, students from the first class must leave and the new class must find their desks, regardless of whether the room holds 10 or 600 people. Here we address the question of how the size of large lecture halls affects classroom-turnover times, focusing on non-emergency settings. By adapting the established social-force model, we treat students as individuals who interact and move through classrooms to reach their destinations. We find that social interactions and the separation time between consecutive classes strongly influence how long it takes entering students to reach their desks, and that these effects are more pronounced in larger lecture halls. While the median time that individual students must travel increases with decreased separation time, we find that shorter separation times lead to shorter classroom-turnover times overall. This suggests that the effects of scheduling gaps and lecture-hall size on classroom dynamics depends on the perspective—individual student or whole class—that one chooses to take.

Keywords: pedestrian dynamics; complex social systems; agent-based modeling; social force; classroom; lecture-hall size

1. Introduction

Pedestrian crowds display complex, nonlinear dynamics [1], and understanding their collective behavior is an active research area [2–6] with early empirical studies dating to over six decades ago [7]. As pedestrians move toward their destinations, they interact with each other, respond to external signals, and account for physical obstacles in their environment, such as a classroom, train, or theater. Understanding how crowds travel through these spaces has applications to design [1,5,8], disease tracing or guidelines [9, 10], evacuation [11–15], crowd management [16], scheduling and route choice [17], and other areas of societal interest. The study of pedestrian crowds is thus interdisciplinary, drawing on fields including biology, sociology, psychology, physics, engineering, computer science, statistics, and mathematics [2, 18–20]. Here we take a mathematical modeling perspective and, motivated by the widespread presence of high-enrollment classes in universities, we focus on student movement and classroom-turnover dynamics in large lecture halls.

Empirical methods for studying pedestrian dynamics include questionnaires [20], observations in the field [21,22], and experiments in lab settings [14,20,23–25]; see [26] for a recent review. Complementing these methods, mathematical approaches to crowd behavior have spanned many techniques, and we highlight the reviews [2–5, 18, 27] (and references therein) for a more extended discussion than we include here. Researchers have developed macroscopic models [28–33] for crowd density and mesoscopic, kinetic-theory models [34–38]. On the microscopic side, prior work includes cellular-automaton [21, 39–45] and lattice-gas models [46–48] that treat pedestrians as individuals moving in discrete space. Off-lattice microscopic models feature differential equations for pedestrian movement and can be velocity- or acceleration-based [3]. Models built on the social-force concept [1, 19, 49]—the framework that we use here—are a prominent off-lattice approach that has been widely studied and adapted (e.g., [12, 16, 50–54]). Researchers have also developed hybrid models [55] and detailed agent-based approaches [56, 57], as well as optimal-control and game-theoretic perspectives [17, 58–64].

Mathematical modeling of crowds often centers on evacuation in venues including airplanes [45], theaters [22, 44], classrooms [40, 41, 46, 56, 57, 65, 66] , and general rooms without internal barriers [39,42,47,67]. By combining experiments with a lattice-gas model, Helbing et al. [46] found a broad distribution of escape times for students in a small, 30-seat classroom. Focusing on a larger room with 168 seats, Fu et al. [65] simulated student movement using a cellular-automaton model. Design questions related to barrier placement, door number, aisle organization, and door width also come up naturally in evacuation studies [1]. For example, Varas et al. [40] tested how different doors affect egress in classrooms of 50–70 seats, and Gao et al. [44] implemented alternative aisle configurations in a theater with 900 seats. In a related vein, Li et al. [15] investigated the effects of exit width on evacuation in classroom environments using a cellular automaton approach.

Across evacuation models and experiments, motion is unidirectional rather than bidirectional: everyone (with the possible exception of emergency workers) seeks to exit the space. The "faster is slower" dynamic [12, 68] can emerge in these settings. This is a phenomenon in which evacuation slows down when pedestrians attempt to move too fast. Another common feature of unidirectional flows, the "zipper effect" occurs when pedestrians stagger themselves as they encounter bottlenecks [24, 25]. On the other hand, bidirectional motion arises in day-to-day environments including transit platforms [7, 16], where models can be used to help address questions surrounding efficiency, route choice, and design. In bidirectional motion, collective dynamics such as lane formation or oscillating flows have been observed

empirically [20] and reproduced in models (e.g., [19, 27, 33, 39, 49, 64, 69, 70]).

Lecture halls in colleges are a venue that combine questions related to evacuation, efficiency, design, and scheduling. Universities also offer unique pedestrian dynamics to investigate since classes can vary in size from under 10 to over 500 people. Despite the associated breadth in room size, there is generally a common scheduling gap between consecutive classes at the same institution. During this break, students from one class must exit and the next class must find their desks. This raises questions about how the time that it takes to empty and fill an academic space is related to lecture-hall size, particularly as universities continue to build or renovate large classrooms [71]. With this motivation, here we address classroom-turnover dynamics in lecture halls of 200 to 600 desks. Unlike prior models of pedestrian dynamics in classrooms (e.g., [15, 40, 46, 65]) that have focused on emergency evacuation or room design for small or moderately-sized classes, we instead directly compare daily movement of entering and exiting students in large classrooms with different capacities. By considering large lecture halls with a broad range of sizes, we take a university-campus level perspective that differs from other studies on emergency evacuation or design in rooms with a fixed capacity. In particular, we use a social-force modeling approach to elucidate how lecture halls of different sizes—and similar design—affect bidirectional student movement and classroom-turnover times in routine, non-emergency settings.

2. Model and methods

To better understand how lecture-hall size is related to classroom-turnover time, we develop an off-lattice model of student dynamics by building on the social-force approach to treat the movement of entering and exiting classes in lecture-hall domains [1, 19, 49]. In the social-force framework [1, 12, 19, 49], general pedestrian "particles" experience acceleration toward their desired velocity, repulsive forces to account for physical obstacles in the domain or interactions with other pedestrians, and possible attractive forces. Importantly, social-force models have been able to replicate many realistic phenomena such as lane and stripe formation [1, 19, 49] or oscillating flows at bottlenecks [19, 49]. Given the flexibility of this off-lattice approach, its widespread use, and its ability to reproduce a range of observed crowd dynamics, we choose it as the basis for student movement in our work. In addition to developing rules for student behavior related to arrival, exit, and finding desks, we adapt the social-force approach to account for forces from realistic obstacles and walls in lecture halls.

Treating each student as an independent agent with their own set of intrinsic features (such as a preferred desk in the classroom), we couple a social-force approach for pedestrian movement with a model of entering and exiting classes that includes rules for how individuals transition between different destinations, such as a door or a desk. We account for heterogeneity in a simplified way by assigning each agent several individual parameters, including a preferred speed, classroom desk, and (depending on if they are entering or exiting the room) an arrival or pre-movement time, among other variables. Informed by the size of large lecture halls at many universities [71–73], we develop several realistic lecture-hall domains, including features such as desks and a vestibule, for student agents to move through in our simulations. In Sections 2.1 and 2.2, we describe how we model lecture-hall spaces and student behavior, respectively. Figure 1 and Table 1 summarize our model and notation. To encourage further work on student dynamics in large lecture halls, all of our code is available on GitLab [74] and our model parameters are given in Table 2 in Section 2.3 and in supplementary material. We discuss how we test the impact of stochasticity in our model on our results in Section 2.4.

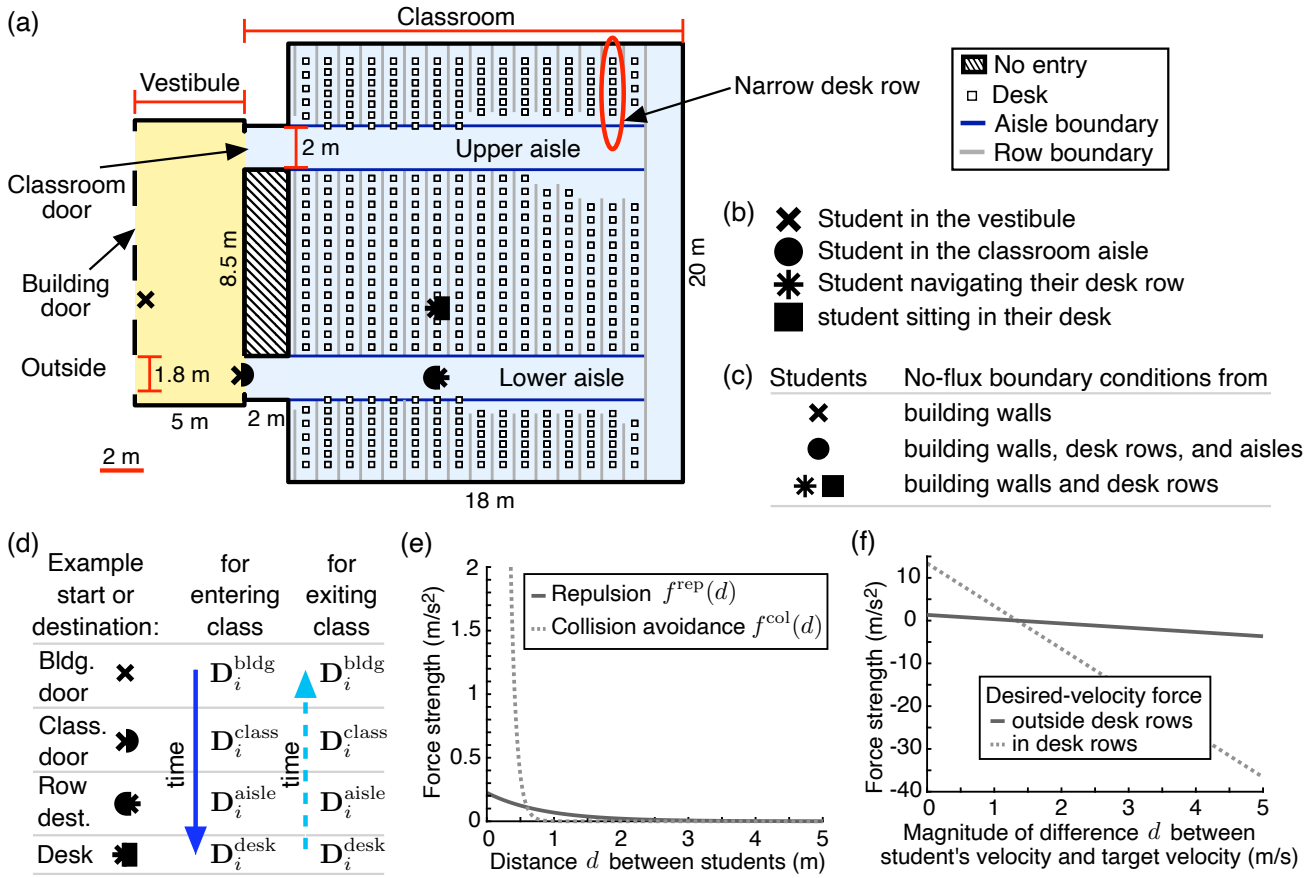

Figure 1. Model overview. (a) We model our baseline domain roughly after our measurements of Rock Hall at the University of California, Davis [72]. We refer to this baseline domain as "our Rock Hall". (b) In our simulations, the symbol shape marking each student's position indicates the region of the building in which the student is located. We consider student i to be in their aisle (desk row) if they are in the classroom with row status $R_i(t) = 0$ ($R_i(t) = 1$); see Section 2.2.1. (c) All students experience no-flux boundary conditions along the building walls and desk rows; students with a row status of zero also experience no-flux conditions along the aisles. (d) As an entering (exiting) student moves toward a desk (building door), their current destination changes. (e) Each student's movement is governed by repulsion from other students and strong local repulsion to model agents not occupying the same space. The maximum of f^{col} is about 140 m/s^2 at $d = 0$. (f) Students feel a force directing them toward their destination and desired speed. To allow pedestrians to make sharp turns when they enter or exit their row of desks, we use a stronger desired-velocity force for students with $R_i(t) = 1$. We plot $\|\mathbf{f}^{\text{des}}(d)\|$ for $v_{\text{avg}} = 1.34$ m/s in Eq (2.13) [75].

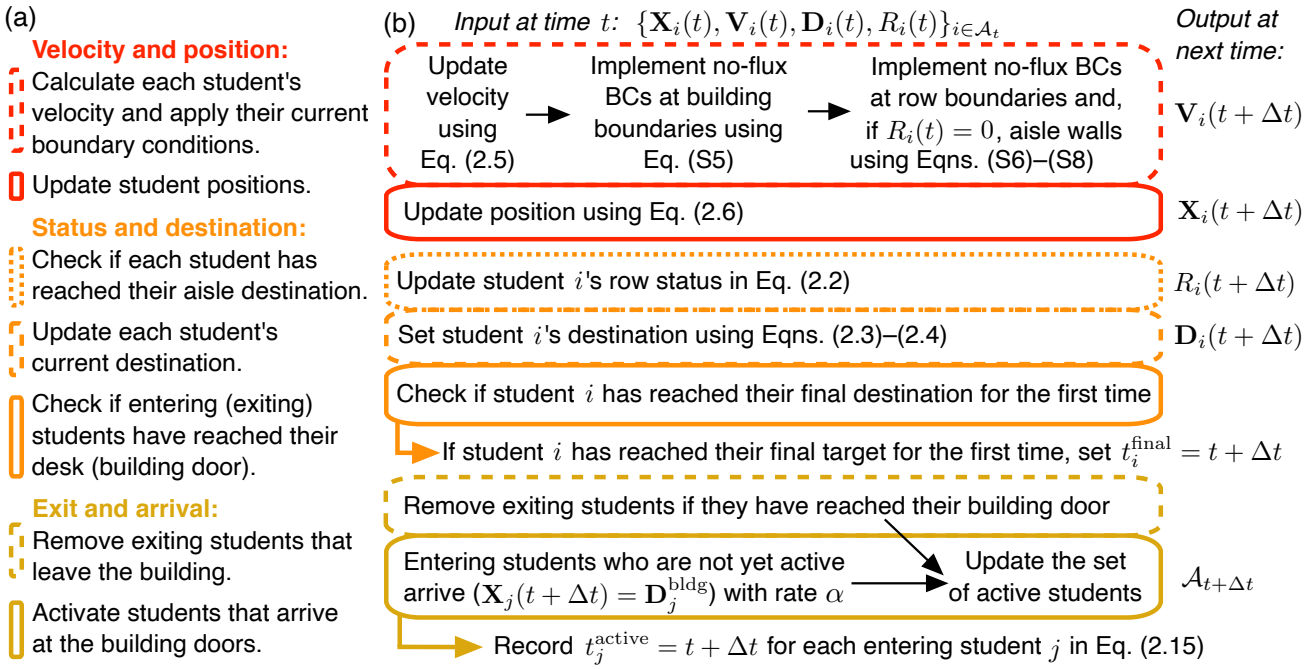

Figure 2. Simulation flowchart. (a) To implement one time step Δt, we follow three main steps. (b) First, we synchronously update the velocity and then the position of each active student (i.e., student in the building) using Eqs (2.5)–(2.6). Second, we check if each student i's row status has changed; update each student's current destination using Eqs (2.3)–(2.4); and log the time t_i^{final} if student i has just reached their final destination. Third, we determine if any new students have arrived to the building; if so, each of these students j is activated (i.e., joins $\mathcal{A}_{t+\Delta t}$) and t_j^{active} is logged. Similarly, we check if any exiting students have reached a building door; if so, we inactivate these students. Equations (S5)–(S8) are in supplementary material.

2.1. Lecture-hall domains

Large universities in the United States frequently have classes with 300 or more students (e.g., see [73] and Supplementary Figure 1), and institutions have continued to build or renovate large lecture halls [71]. We construct our baseline domain after Rock Hall at the University of California, Davis. Rock Hall has functioned as a movie theater and a concert hall, but it is now used mainly for high-enrollment classes. Rock Hall (Supplementary Figures 1(c)–(d)) can accommodate 416 people and is a good example of a generic large classroom. As we show in Figure 1(a), our baseline domain—i.e., "our Rock Hall"—has a vestibule with four external doors and a classroom with two doors and two aisles.

In addition to our baseline domain, we develop four other lecture-hall domains of different sizes; see Supplementary Figure 2. In particular, in Section 3.3, we investigate how lecture-hall size affects classroom-turnover times. To do so, we adapt our baseline domain to construct smaller and larger rooms, spanning 200 to 600 desks (Supplementary Figure 2). Because our focus is on size rather than design, we make minimal changes to the room geometry and instead accommodate more students by adding more rows of desks and increasing the length of the room from classroom door to the last row of desks nearest the instructor. See supplementary material for more details.

2.2. Student dynamics

We model each student as an agent with seven intrinsic features and four time-dependent variables as below:

$$\text{student } i = \{\underbrace{C_i, \tau_i^{\text{pre}}, v_i^{\text{des}}, \mathbf{D}_i^{\text{bldg}}, \mathbf{D}_i^{\text{class}}, \mathbf{D}_i^{\text{aisle}}, \mathbf{D}_i^{\text{desk}}}_{\text{time-independent features}}, \underbrace{\mathbf{X}_i(t), \mathbf{V}_i(t), \mathbf{D}_i(t), R_i(t)}_{\text{time-dependent variables}}\}, \tag{2.1}$$

where C_i denotes student i's class (entering or exiting); τ_i^{pre} is the time that it takes student i to prepare to leave their desk (if they are in the exiting class); v_i^{des} is their desired speed; $\mathbf{D}_i^{\text{bldg}}$, $\mathbf{D}_i^{\text{class}}$, $\mathbf{D}_i^{\text{aisle}}$, and $\mathbf{D}_i^{\text{desk}}$ correspond to student i's desired building door, classroom door, aisle destination, and desk, respectively; $\mathbf{X}_i(t)$ is their position; $\mathbf{V}_i(t)$ is their velocity; $\mathbf{D}_i(t)$ is their current destination; and $R_i(t)$ is a status variable that logs whether or not student i is in a desk row. Figure 2 overviews how we update student i's time-dependent features.

We assume that there are $N^{\text{enter}} \geq 0$ and $N^{\text{exit}} \geq 0$ students in the entering and exiting classes, respectively. We let $\mathcal{A}_t \subset \{1, ..., N^{\text{enter}} + N^{\text{exit}}\}$ be the set of students who are in the building (or "active") at time t, and we only track this set of active students in our simulations (Figure 1(a)). Our model of student behavior then includes three main components: differential equations for agent movement in lecture-hall domains (Section 2.2.2), discrete-time rules for arrival and exit at the building doors (Section 2.2.3), and discrete-time rules that govern how each student i's current target $\mathbf{D}_i(t)$ is selected from among $\mathbf{D}_i^{\text{bldg}}$, $\mathbf{D}_i^{\text{class}}$, $\mathbf{D}_i^{\text{aisle}}$, and $\mathbf{D}_i^{\text{desk}}$ and how their row status $R_i(t)$ evolves (Section 2.2.1). As initial conditions, we assume that each student i in the exiting class starts at a desk with zero velocity. Once active, entering students begin with zero velocity at one of the building doors. We also allow $N^{\text{early}} \geq 0$ entering students to start in the vestibule. See supplementary material for details about our initial conditions.

To account for some variability, we assign each student i a pre-movement time τ_i^{pre} and desired speed v_i^{des}. We draw the desired speeds from a normal distribution with mean $v_{\text{avg}} = 1.34$ meters per second (m/s) and standard deviation $v_{\text{std}} = 0.37$ m/s; these values are based on prior studies [1, 23, 49, 54, 70, 75]. To our knowledge, data on the time that it takes people to gather their belongings and prepare to move after a lecture in non-emergency settings is limited. Notably, Zhang et al. [66] track pre-movement times in classrooms during evacuation experiments. The study [22] also provides pre-movement times for evacuations in a theater. Motivated in part by the distributions in [22], we sample τ_i^{pre} for exiting students from a normal distribution with mean $\mu_{\text{pre}} = 35$ s and standard deviation $\sigma_{\text{pre}} = 20$ s. We set $\tau_i^{\text{pre}} = 0$ for entering students. In practice, we truncate the distribution for v_i^{des} at one standard deviation from the mean, and we implement cutoffs for τ_i^{pre} to ensure this delay time is positive and no longer than 2 minutes.

2.2.1. Student destinations

In our model, entering students become active at building doors and have a final goal of reaching the position of their desk ($\mathbf{D}_i^{\text{desk}}$). Each exiting student i starts at a desk and has a building door ($\mathbf{D}_i^{\text{bldg}}$) from which they seek to exit. At the start of a simulation, we assign desks and building doors to pedestrians uniformly at random from the set of desks and four building doors, respectively; see Figure 1(a). However, if a student immediately moved toward their desk when they entered the building, they would

attempt to travel through walls. We thus introduce two intermediate destinations, and student i's current target $\mathbf{D}_i(t)$ changes as they move through space.

As we show in Figure 1(d), if student i is in the entering class and has arrived to the building, their first destination is $\mathbf{D}_i^{\text{class}}$, corresponding to the internal door that they will use to enter the classroom. Their next target is $\mathbf{D}_i^{\text{aisle}}$, the location in the center of the aisle associated with their desired row of desks. Once student i has reached this "aisle destination", their final target is the coordinates of their desk, namely $\mathbf{D}_i^{\text{desk}}$. Similarly, if student i is in the exiting class, their first target is $\mathbf{D}_i^{\text{aisle}}$. Once they have exited their row of desks, student i seeks to move toward their classroom door ($\mathbf{D}_i^{\text{class}}$) and then their building door ($\mathbf{D}_i^{\text{bldg}}$). Importantly, $\mathbf{D}_i^{\text{class}}$ and $\mathbf{D}_i^{\text{aisle}}$ depend on $\mathbf{D}_i^{\text{desk}}$: we assume students use the classroom door and travel in the aisle closest to their desk. See supplementary material for details.

To select $\mathbf{D}_i(t)$ from $\mathbf{D}_i^{\text{bldg}}$, $\mathbf{D}_i^{\text{class}}$, $\mathbf{D}_i^{\text{aisle}}$, and $\mathbf{D}_i^{\text{desk}}$, we introduce a status variable that tracks whether or not student i has reached $\mathbf{D}_i^{\text{aisle}}$, as below:

$$R_i(t) = \begin{cases} 1 & \text{if student } i \text{ is in their narrow desk row} \\ 0 & \text{otherwise.} \end{cases} \tag{2.2}$$

The row status of each student in the entering (exiting) class starts at zero (one) and changes to one (zero) once they reach their aisle destination. Student i has reached their aisle destination when $\|\mathbf{X}_i(t) - \mathbf{D}_i^{\text{aisle}}\| < d_{\text{tol}}$, where $d_{\text{tol}} = 0.3$ m is a tolerance distance and $\|\mathbf{x}\| = \sqrt{x_1^2 + x_2^2}$. We then update $\mathbf{D}_i(t)$ as follows:

$$\mathbf{D}_i(t) = \begin{cases} \mathbf{D}_i^{\text{class}} & \text{if } i \text{ is not inside the classroom} \\ \mathbf{D}_i^{\text{aisle}} & \text{if } i \text{ is in the classroom and } R_i(t) = 0 \\ \mathbf{D}_i^{\text{desk}} & \text{otherwise.} \end{cases} \tag{2.3}$$

See Figure 1(a). Similarly, for each student i in the exiting class, we specify their current destination as below:

$$\mathbf{D}_i(t) = \begin{cases} \mathbf{D}_i^{\text{aisle}} & \text{if } R_i(t) = 1 \ (i \text{ is in their desk row}) \\ \mathbf{D}_i^{\text{class}} & \text{if } R_i(t) = 0 \text{ and } i \text{ is in the classroom} \\ \mathbf{D}_i^{\text{bldg}} & \text{otherwise.} \end{cases} \tag{2.4}$$

We update $R_i(t)$ and $\mathbf{D}_i(t)$ as appropriate at each time step $\Delta t = 0.01$ s. As we discuss next in Section 2.2.2, $\mathbf{D}_i(t)$ and $R_i(t)$ play a role in student movement.

Table 1. Our notation; see Figures 1 and 2 for a model overview and flowchart, respectively.

Notation	Meaning
$\mathcal{A}_t$	set of students that are in the building (i.e., active) at time t
τ_i^{pre}	time that exiting student i takes to prepare to leave their desk (if i is in the entering class, $\tau_i^{\text{pre}} = 0$)
v_i^{des}	student i's desired speed
$\mathbf{D}_i^{\text{bldg}}$	entering student i's initial condition or exiting student i's final target (a building door to outside; see Figure 1(d))
$\mathbf{D}_i^{\text{class}}$	coordinates of internal door (between vestibule and classroom) that student i uses
$\mathbf{D}_i^{\text{aisle}}$	student i's desired destination in the aisle near their row of desks
$\mathbf{D}_i^{\text{desk}}$	exiting student i's initial condition or entering student i's final target (a desk in the classroom)
$\mathbf{X}_i(t)$	position of student i at time t
$\mathbf{V}_i(t)$	velocity of student i at time t
$\mathbf{D}_i(t)$	current destination of student i at time t ($\mathbf{D}_i^{\text{bldg}}$, $\mathbf{D}_i^{\text{class}}$, $\mathbf{D}_i^{\text{aisle}}$, or $\mathbf{D}_i^{\text{desk}}$, depending on their location and class); see Eqs (2.3)–(2.4)
$R_i(t)$	row status of student i at time t ($R_i(t) = 1$ if student i is in their narrow desk row and 0 otherwise)
t_i^{active}	time that student i is first active (in the building)
t_i^{final}	time that student i first reaches their final destination

2.2.2. Student movement

We describe student movement through a social-force modeling approach [1, 19, 49]. This model treats pedestrians as particles that react to social forces. Pedestrians do not want to bump into other agents, so they feel a repulsive force from other individuals. At the same time, pedestrians experience attractive forces toward their destinations. For each active student $i \in \mathcal{A}_t$, the evolution of their position $\mathbf{X}_i(t)$ and velocity $\mathbf{V}_i(t)$ is given by:

$$d\mathbf{V}_i(t) = \begin{cases} \underbrace{\sum_{j\in\mathcal{A}_t, j\neq i} \mathbf{f}^{\text{col}}(\mathbf{x}_{ij})dt}_{\text{collision avoidance}} + \underbrace{\sum_{j\in\mathcal{A}_t, j\neq i} \mathbf{f}^{\text{rep}}(\mathbf{x}_{ij}, \mathbf{v}_{ij})dt}_{\text{student repulsion}} + \underbrace{\mathbf{f}^{\text{des}}(\mathbf{D}_i - \mathbf{X}_i, \mathbf{V}_i, v_i^{\text{des}}, R_i)dt}_{\text{desired velocity}} + \underbrace{\sigma d\mathbf{W}^i(t)}_{\text{stochasticity}} & \text{if } t \geq \tau_i^{\text{pre}} \\ 0 & \text{otherwise,} \end{cases} \tag{2.5}$$

$$\frac{d\mathbf{X}_i}{dt}(t) = \mathbf{V}_i(t), \tag{2.6}$$

where $\mathbf{W}^i$ is a Wiener process; σ is the noise strength; τ_i^{pre} is student i's pre-movement time ($\tau_i^{\text{pre}} = 0$ if i is in the entering class); and the forces $\mathbf{f}^{\text{col}}$ and $\mathbf{f}^{\text{rep}}$ depend on the difference between student positions (centers of mass) $\mathbf{x}_{ij} = \mathbf{X}_i - \mathbf{X}_j$ and between their velocities $\mathbf{v}_{ij} = \mathbf{V}_i - \mathbf{V}_j$.

The force $\mathbf{f}^{\text{col}}$ operates strongly over a short distance to prevent collisions, and $\mathbf{f}^{\text{rep}}$ acts weakly over a longer range to help students maintain a comfortable distance from one another. These forces can be

expressed in terms of potentials U^{rep} and U^{col} (see Eq. (2.12)) as below:

$$\begin{aligned} \mathbf{f}^{\text{col}}(\mathbf{x}) &= -\nabla_{\mathbf{x}} U^{\text{col}}(\xi_{\text{C}}(\mathbf{x})), \\ \mathbf{f}^{\text{rep}}(\mathbf{x}, \mathbf{v}) &= -\nabla_{\mathbf{x}} U^{\text{rep}}(\xi_{\text{E}}(\mathbf{x}, \mathbf{v}\delta_t)), \end{aligned} \tag{2.7}$$

where $\xi_{\text{C}}(\mathbf{x}_{ij})$ and $\xi_{\text{E}}(\mathbf{x}_{ij}, \mathbf{v}_{ij}\delta_t)$ correspond to the perceived distance between individuals i and j. These distances can depend on the current difference between their positions ($\mathbf{x}_{ij}$) and on the projected difference in their future positions ($\mathbf{x}_{ij} + \mathbf{v}_{ij}\delta_t$) over a timescale δ_t, assuming that $\mathbf{v}_{ij}$ is constant on the time interval $[t, t + \delta_t)$.

Following the example of [19, 53], we use two methods for specifying the interaction forces between students: one depends only on the current distance between their positions ("the circular force specification") and the other accounts for their current and projected future positions ("the elliptical force specification"). The circular distance is $\xi_C(\mathbf{x}) = ||\mathbf{x}||$, and the elliptical distance is given by:

$$\xi_{\text{E}}(\mathbf{x}, \mathbf{v}\delta_t) = \frac{\sqrt{(||\mathbf{x}|| + ||\mathbf{x} + \mathbf{v}\delta_t||)^2 - ||\mathbf{v}\delta_t||^2}}{2}. \tag{2.8}$$

As we introduced in Eq (2.7), we define the repulsive forces in our model by taking the gradient of the potentials U^{***} with respect to $\mathbf{x}$ [49], which yields the following expressions:

$$\begin{aligned} \mathbf{f}^{\text{col}}(\mathbf{x}) &= f^{\text{col}}(\xi_{\text{C}}(\mathbf{x}))\nabla_{\mathbf{x}}\xi_{\text{C}}(\mathbf{x}), \\ \mathbf{f}^{\text{rep}}(\mathbf{x}, \mathbf{v}) &= f^{\text{rep}}(\xi_{\text{E}}(\mathbf{x}, \mathbf{v}\delta_t))\nabla_{\mathbf{x}}\xi_{\text{E}}(\mathbf{x}, \mathbf{v}\delta_t), \end{aligned} \tag{2.9}$$

where, given Eq (2.8), the gradients of $\xi_*(\cdot)$ are given by:

$$\nabla_{\mathbf{x}}\xi_{\text{C}}(\mathbf{x}) = \frac{\mathbf{x}}{||\mathbf{x}||} \tag{2.10}$$

$$\nabla_{\mathbf{x}}\xi_{\text{E}}(\mathbf{x}, \mathbf{v}\delta_t) = \frac{||\mathbf{x}|| + ||\mathbf{x} + \mathbf{v}\delta_t||}{2\sqrt{(||\mathbf{x}|| + ||\mathbf{x} + \mathbf{v}\delta_t||)^2 - ||\mathbf{v}\delta_t||^2}} \left(\frac{\mathbf{x}}{||\mathbf{x}||} + \frac{\mathbf{x} + \mathbf{v}\delta t}{||\mathbf{x} + \mathbf{v}\delta_t||} \right), \tag{2.11}$$

and

$$f^{***}(x) = B^{***} e^{(r-x)/b^{***}}. \tag{2.12}$$

Here B^{***} is related to the force strength; b^{***} is the interaction range; $^{***} \in \{\text{col}, \text{rep}\}$ indicates that we use different parameters [53] for each force (see Figure 1(e) and Table 2); and $r = 0.6$ m is the diameter of the privacy sphere that pedestrians seek to maintain [1]. When $\delta_t = 0$ s, Eq (2.11) simplifies to Eq (2.10) and $\mathbf{f}^{\text{rep}}$ has the same form as $\mathbf{f}^{\text{col}}$ in Eq (2.9). The elliptical model specification ($\delta_t > 0$) allows pedestrian interactions to depend on relative velocity as well as on distance, and it enables the repulsive force to have a lateral component. As a consequence, this approach leads to smoother, less confrontational pedestrian behavior [19, 53]. We use $\delta_t = 0.1$ s, which is similar to values used in [19].

Lastly, to account for each student's current destination, we specify that agent $i \in \mathcal{A}_t$ feels an attractive force [49, 53] in the direction of $\mathbf{d} = \mathbf{D}_i(t) - \mathbf{X}_i(t)$:

$$\mathbf{f}^{\text{des}}(\mathbf{d}, \mathbf{v}, v^{\text{des}}, R) = \begin{cases} \frac{1}{\tau}\left(v^{\text{des}} \frac{\mathbf{d}}{||\mathbf{d}||} - \mathbf{v} \right) & \text{if } R \neq 0 \\ \frac{1}{\tau_{\text{row}}}\left(v^{\text{des}} \frac{\mathbf{d}}{||\mathbf{d}||} - \mathbf{v} \right) & \text{if } R = 0 \end{cases}, \tag{2.13}$$

where $\{\tau, \tau_{\text{row}}\}$ are the relaxation times in which students adapt their velocity $\mathbf{V}_i(t)$ to move toward their current destination $\mathbf{D}_i(t)$ with speed v; $R \neq 0$ means the student is not in a desk row; and $R = 0$ means the student is in a desk row. Similar to prior studies [1, 49], we choose a baseline relaxation time of $\tau = 1$ s. However, we find that students need to make sharper adjustments to their velocity when turning into (or out of) their desk row and navigating the narrow rows of the classroom. Following the example in [49], we thus set $\tau_{\text{row}} = 0.1$ s for entering (exiting) students who have reached (not yet left) the row of their desired desk.

We implement no-flux boundary conditions along the building outline. We also treat the boundaries of the desk rows as physical walls to model desks that are too close together for students to move between rows; see Figure 1. Additionally, if $R_i(t) = 0$ in Eq (2.2), we include no-flux boundary conditions along the aisle boundaries. This models our assumption that entering students do not want to step out of the aisle unless they have arrived at their desk row. See supplementary material for more information.

2.2.3. Student arrival and exit

At each time step Δt, if the entire entering class is not yet in the building, students arrive at the doors stochastically with rate α. In particular, if entering student $i \notin \mathcal{A}_t$, then $i \in \mathcal{A}_{t+\Delta t}$ with probability

$$p = \frac{\alpha \Delta t}{\text{number of entering students not yet active}}. \tag{2.14}$$

Once all of the entering students are active, no new students enter the building. We define the time that each student i first becomes active as

$$t_i^{\text{active}} = \text{earliest time that } i \text{ is in the building}, \tag{2.15}$$

and we note that $t_i^{\text{active}} = 0$ s for each exiting student i, since these students begin in the classroom. For our simulations with only an entering class, we also include $N^{\text{early}} > 0$ students who start active in the vestibule; when we include an exiting class, we use $N^{\text{early}} = 0$.

Students from the exiting class become inactive and are removed from our simulation when they are within a tolerance distance d_{tol} of their assigned building door ($\mathbf{D}_i^{\text{bldg}}$ for student i) or have left the building. Entering students, on the other hand, are active from the time of their arrival onward. We define

$$t_i^{\text{final}} = \text{time that } i \text{ reaches their final destination}, \tag{2.16}$$

where this is the time that entering students first reach their desks and exiting students exit the building (or reach a distance d_{tol} from their desired building door). If a student does not reach their final target during our simulation, we set $t_i^{\text{final}} = t_{\max} + 1$, where $t_{\max}$ is the total simulation time.

Table 2. Parameters. See supplementary material for values that are simulation-specific by figure.

Parameter	Value	Motivation and meaning
v_{avg}	1.34 m/s	Mean speed at which students desire to move [49, 75]
v_{std}	0.37 m/s	Standard deviation for the students' desired speed [75]
τ	1.0 s	Relaxation timescale for the force that students outside of desk rows feel to align with their desired velocity (Eq (2.13)) [1]
τ_{row}	0.1 s	Relaxation timescale for the force that aligns students in desk rows with their desired velocity (Eq (2.13)); less than τ to allow for quick changes in velocity in desk rows
δ_t	0.1 s	Timescale for how far in advance students can predict the movement of others (Eqs (2.8)–(9)); similar to choice in [19]
B^{rep}	0.11 m/s^2	Repulsion strength to maintain a comfortable distance between pedestrians (Eq (2.12)) [53]
b^{rep}	0.84 m	Interaction range for repulsive force (Eq (2.12)) [53]
B^{col}	0.11 m/s^2	Repulsion strength in the collision-avoidance force (Eq (2.12)); chosen equal to B^{rep}
b^{col}	0.084 m	Interaction range for collision-avoidance force (Eq (2.12)); chosen to be $0.1B^{\text{rep}}$
r	0.6 m	Diameter of pedestrian privacy sphere (Eq (2.12)) [1]
σ	0.001 m/s$^{3/2}$	Noise strength in the differential equation for student velocity (Eq (2.5)); chosen to include weak noise
μ	0.01 m	Small amount of noise in $\mathbf{D}_i^{\text{class}}$ for entering student i (supplementary material); helps prevent rare head-on collisions in the vestibule
N^{enter}	Varies	Number of students in the entering class
N^{early}	Varies	Number of students who are in $\mathcal{A}_0$ and start in the vestibule
N^{exit}	Varies	Number of students in the exiting class
t_{sep}	Varies	Time in seconds between when the first class ends and when entering students begin arriving (range of values tested)
d_{tol}	0.3 m	Tolerance distance when updating row status and t^{final} (Eq (2.16)–(3.1)); chosen to be $r/2$
b_{bnd}	0.6 m	Distance from the building walls in which velocity is reduced for boundary conditions (supplementary material); chosen to be r
b_{tight}	0.3 m	Distance from doors, aisle walls, or desk-row walls in which velocity is reduced for boundary conditions (supplementary material); chosen less than b_{bnd} to accommodate movement in tight spaces
α	$0.004175N^{\text{enter}}$ students/s	Rate of entering students arriving at the building doors (Eq (2.14)); chosen so that the class arrives over about 4 minutes
μ_{pre}	60 s	Mean pre-movement time for exiting students; informed by [22]
σ_{pre}	35 s	Standard deviation in the pre-movement times for exiting students; informed roughly by [22]
$\lambda_{\text{min}}^{\text{pre}}$	0 s	Cutoff parameter in our distribution for τ_i^{pre}; chosen so exiting students do not leave before class ends
$\lambda_{\text{max}}^{\text{pre}}$	120 s	Cutoff parameter in our distribution for τ_i^{pre}; chosen to be $2\mu_{\text{pre}}$

2.3. Model parameters

We include all of our model parameters in Table 2. To support the reproducibility of our work, we also list the simulation-specific values of N^{enter}, N^{exit}, N^{early}, and t_{sep} by figure in supplementary material.

2.4. A-test analysis

Our model includes several stochastic features, such as each student's initial position and final destination (e.g., desired desks for the entering class). Uncertainty quantification is helpful to determine the number of simulations needed to capture the variance in the summary statistics that we use to describe our results, as shown in [76–78]. We perform this analysis using the A-test measure, as described in [79]. The A-test involves completing 20 sets of k simulations each with the same parameters, and extracting a relevant measure for describing the simulations. Each set from 1 to 20 is then compared with set 1 based on this measure to return an A-score, which represents the probability that a randomly selected sample from the first population is larger than a random sample from the second population [80]. More specifically, the score $A_{i,j}$ compares sets i and j to determine the significance of the sample size k of simulations within each set. Following the approach in [79], we compute the discrete approximation of the A-score as:

$$A_{i,j} = \frac{\#(X_m > Y_n)}{k^2} + 0.5\frac{\#(X_m = Y_n)}{k^2}, \tag{2.17}$$

where $m, n = 1, \ldots, k$ and $\#(X_m > Y_n)$ is the number of times an element (measure X_m) in set i is greater than an element (measure Y_n) in set j, for all X_m's in set i and all Y_n's in set j. Similarly, $\#(X_m = Y_n)$ is the number of times an element (X_m) in set i is equal to an element (Y_n) in set j. Sets i and j each consist of k simulations.

Figure 3 shows the A-score for 20 sets of our baseline entering simulations (Figures 4 and 5), with sample sizes ranging from $k = 50$ to $k = 100$ and using the parameter values in Table 2. We use the mean time that it takes students to reach their seat as our measure to compute the A-scores. The results in Figure 3 are based on k simulations of 400 students entering our Rock Hall. The different lines in Figure 3 provide a means of interpreting test results: scores above 0.71 or below 0.29 (outside the dot-dashed lines) mark a large effect of the sample size k on the model results; scores above 0.64 or below 0.36 (outside the dotted lines) indicate a medium effect of the sample size k on the results, and scores between 0.44 and 0.56 (within the solid lines) illustrate a small effect on the model results. Therefore, the closer the A-score is to 0.5 for the set comparisons, the smaller the effect that the number of simulations k has on the mean travel time for entering students in our model. An A-score of exactly 0.5 corresponds to no effect of k on the model results. Note that $A_{1,1} = 0.5$, since set 1 is compared to itself, which provides validation for our A-test analysis.

As the number of simulations increases from 50 (Figure 3(a)) to 100 (Figure 3(c)), we find that the number of scores $A_{i,j}$ falling within the solid lines increases. This shows that as the number of simulations k increases, the impact of stochastic factors on our results decreases. In Figure 3(c), where each set contains $k = 100$ simulations, we find that all of the A-scores—except for one—fall within the solid line interval closest to 0.5. This means that $k = 100$ simulations are sufficient to capture most of the variance driven by the stochastic elements in our model. With the exception of the example simulations in Figures 4, 6(d)–(h), 7(d)–(h) and Supplementary Figure 3, all of our results are thus based on summary statistics calculated across 100 simulations.

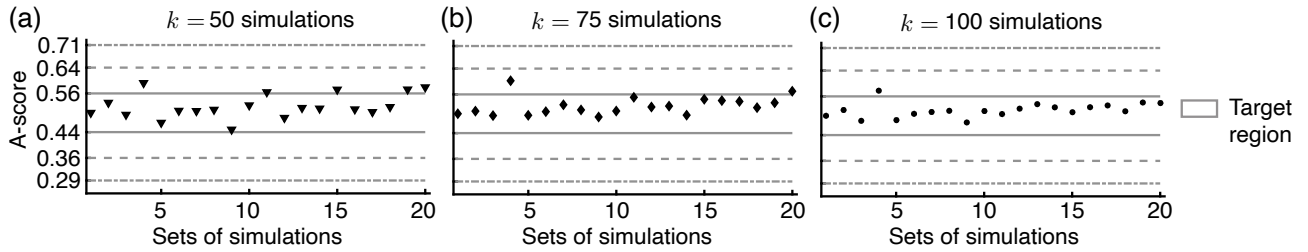

Figure 3. A-test analysis of our model for the case of 400 students entering our Rock Hall with no exiting class. We show the A-score, computed using student travel times, for (a) 50, (b) 75, and (c) 100 simulations. At $k = 100$, all of the A-scores but one fall within the target region (solid lines), so we base our results on 100 simulations under each condition.

3. Results

Using our model from Section 2.2, we now present a study of the effects of lecture-hall size on classroom-turnover times. We discuss our results in terms of two time quantities, both measured in seconds: the simulation time t and the travel time of individual students. When there is an exiting class present, $t = 0$ s is the time when this first class ends. Understanding how long it takes all of the entering students to reach their desks measured from $t = 0$ s thus provides information about classroom-turnover times. From a single student i's perspective, we also find it useful to define their travel time from building door to desk (or vice versa), namely

$$t_i^{\text{trav}} = t_i^{\text{final}} - t_i^{\text{active}}, \tag{3.1}$$

where t_i^{active} and t_i^{final} are defined in Eqns. (2.15)–(2.16), respectively.

In Section 3.1, we begin with a baseline study of how quickly an entering (exiting) class of students can reach their desks (leave the building) in the absence of another class. This models dynamics in the first or last class of the day, respectively. In Section 3.2, we consider two classes, scheduled consecutively, in the same lecture hall. Lastly, in Section 3.3, we test the effects of lecture-hall size on classroom-turnover times. Our results indicate that lecture-hall size and the time between consecutive classes work together to control how long it takes students to exit the classroom or reach their desks.

3.1. Baseline: our Rock Hall with one class

To establish a baseline for our model, we first simulate 400 students entering our Rock Hall domain, with no exiting class. Figure 4 shows time snapshots of students entering the classroom, as well as summary statistics of pedestrian dynamics. The students' mean speed is close to their average desired velocity in the vestibule, and it decreases with time as students reach their desks (Figure 4(a)). Similarly, students are relatively spread out in the vestibule, but the mean distance between nearest-neighboring students eventually decreases to the distance between desks (Figure 4(b)). We provide the distribution of student travel times t_i^{trav} in Figure 4(c).

Since our model is stochastic, we also investigate if these trends are consistent across multiple simulations. In Section 2.4, we described the A–test method for uncertainty quantification based on [79]; also see Eq (2.17). Using this method, we find that 100 simulations of our model are sufficient to mitigate the uncertainty introduced by stochastic model elements on the mean student travel time in

Eq (3.1). For the remainder of our paper, we therefore show summary statistics based on 100 simulations for our results, with the exception of sample simulation snapshots.

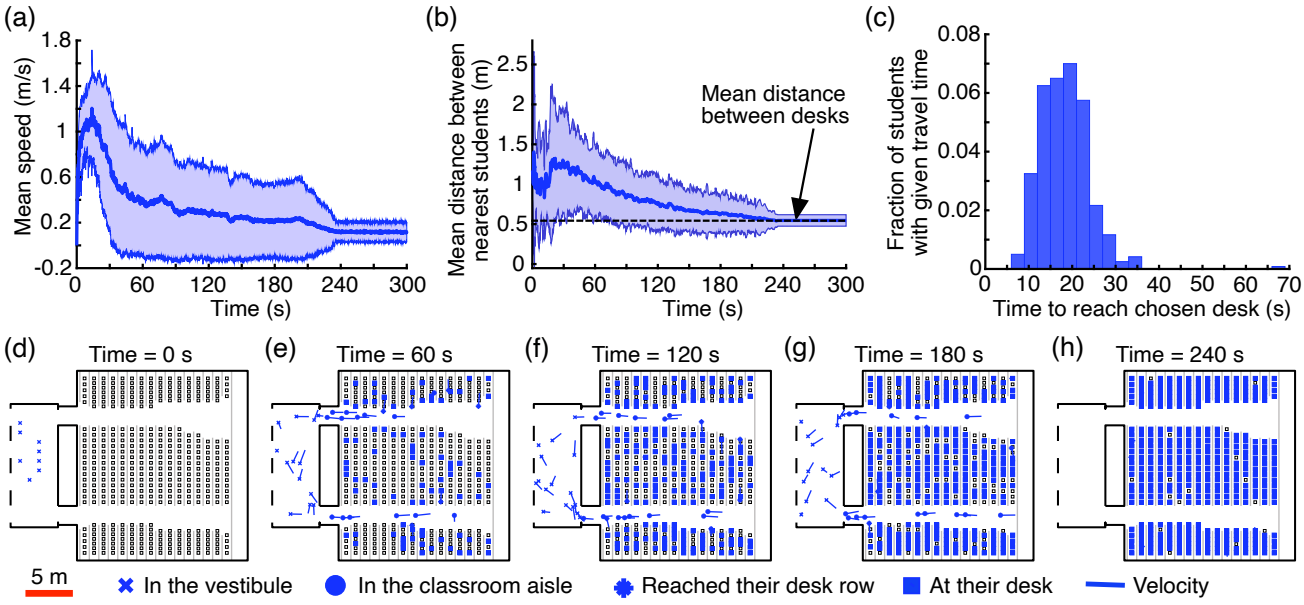

Figure 4. Example simulation of 400 students entering our Rock Hall, with no exiting class. (a) We show the mean speed of active students through time for a representative simulation. (b) As time (from the start of the simulation) passes, the mean distance between nearest students approaches the average distance between desks. In panels (a)–(b), solid lines denote the mean, and shaded areas indicate the standard deviation over all active students at each time point. (c) The distribution for the time (i.e., t_i^{trav} for student i) that it takes students to travel from a building door to their desk is right-skewed. Our histogram bin width is 3 s. (d)–(h) We show positions and velocities of students at five time points for an example simulation.

Figure 5(a)–(c) display speeds and student–student distances across 100 simulations of 400 entering students in our Rock Hall. Across our 100 simulations, all of the students reach their desks by the total simulation time ($t_{\max} = 280$ s). However, we find that 36 students take longer than 100 s to reach their desk, which can occur when they enter the wrong desk row. This amounts to 0.9% of the total number of students in these simulations, and as a result we crop the long tail in our travel-time distributions in Figure 5(c). We similarly observe very low percentages of stuck pedestrians in other simulation settings, where we again omit these students from our figures; see supplementary material for details.

We next simulate 400 students exiting Rock Hall, with no entering class. Figure 6 shows summary statistics across 100 simulations, as well as time snapshots for an example simulation. The mean speed of exiting students in Figure 6(a) behaves opposite to that of entering students in Figure 5(a). Students initially move slowly as they navigate tight rows and crowded aisles, and they later approach their desired speed. The mean distance between neighboring students is initially determined by the spacing between desks, but it increases as students leave their desks (Figure 6(b)). As more students exit the building, the standard deviation in student–student distance increases, since it is calculated over a smaller number of agents. The time that it takes students to exit appears to roughly follow a normal distribution; see Figure 6(c). As we discuss in Section 2.2, we model the amount of time τ_i^{pre} that students take to

gather their belongings by a truncated normal distribution with parameters in Table 2. The travel-time distribution is, as we would expect, a shifted version of this distribution of pre-movement times.

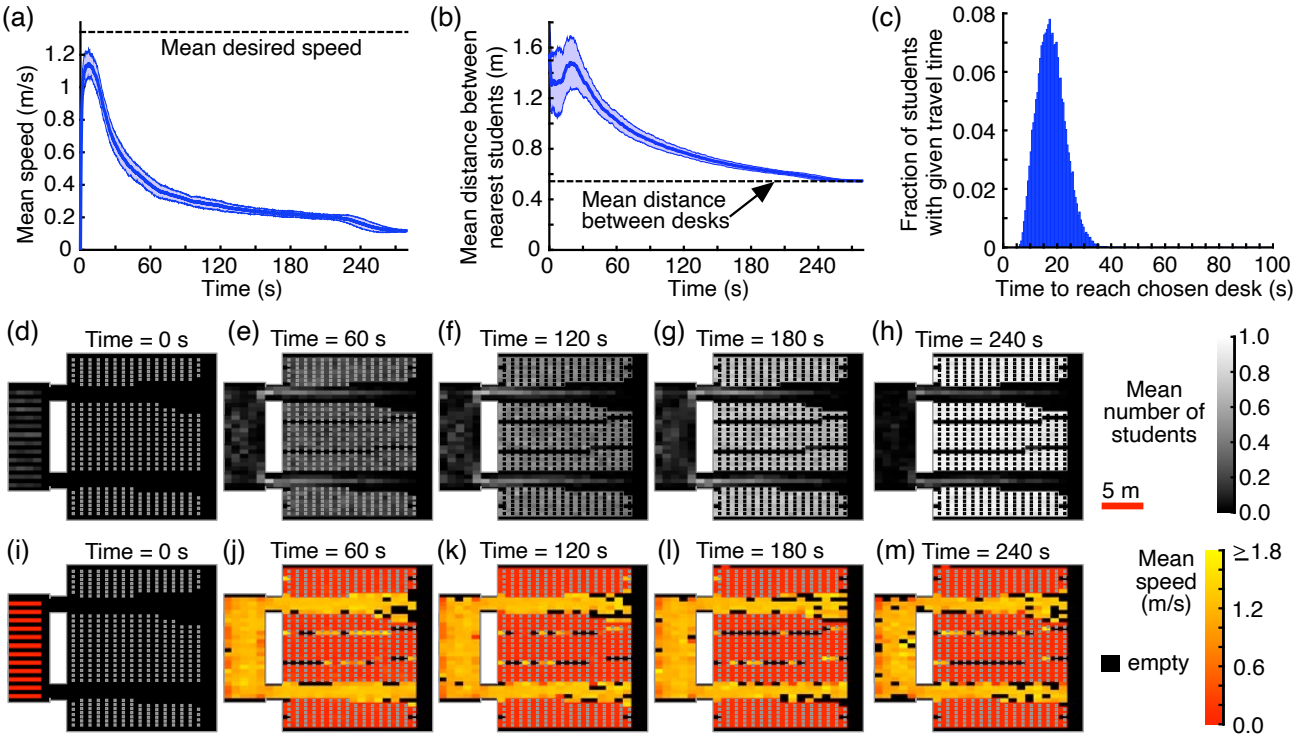

Figure 5. Entering class of 400 students in our Rock Hall, with no exiting class. All panels present summary statistics across 100 simulations. In agreement with Figure 4, the (a) mean speed and (b) mean distance between nearest students decays in time. In panels (a)–(b), solid (shaded) lines are the mean (standard deviation) across 100 simulations. (c) We show the travel-time distribution for all students across 100 simulations. The histogram bin width is 0.5 s, and we crop the long tail in the distribution at 100 s; a few outlier agents (about 0.9% of the total number of students across 100 simulations) take a longer time to reach their desks. For comparison with Figures 4(d)–(h), we show in (d)–(h) mean mass (number of students in grid squares with area 1.5 m^2) and (i)–(m) associated mean speed in those grid squares across 100 simulations at five time points; see supplementary material. Each grid square contains at most one desk, and desk positions are indicated as gray or black squares. Note $N^{\text{entering}} > 0$ students start in the vestibule, visible in panels (d) and (i). In panels (l)–(m), most students have reached their desks, so the velocities are means across a limited number of agents.

3.2. Our Rock Hall with both entering and exiting classes

Scheduling consecutive classes in the same lecture hall is likely to impact student travel times. To investigate this, we consider bidirectional simulations in our Rock Hall. Specifically, we model $N^{\text{exiting}} = 400$ students who begin to exit the lecture hall at the end of their class, and $N^{\text{entering}} = 400$ students who start arriving to the building for the next class. We specify a separation time $t_{\text{sep}} = 90$ s between the end of the first class and the time when students in the next scheduled class begin to arrive at the building doors. For all of our simulations with both entering and exiting classes, we set $N^{\text{early}} = 0$,

so there are no students who start in the vestibule.

We show summary statistics across 100 simulations in Figure 7, as well as time snapshots illustrating how students from the two classes interact in an example simulation. Prior to the separation time of 90 s, only exiting students are active. As students in the entering class begin to arrive at the building doors, we observe more interactions between the two classes, especially in the vestibule and at the classroom doors. Once all of the exiting students have left the building, entering students are the only pedestrians present. In our model implementation, these observations correspond to changes in the set of active students $\mathcal{A}_t$. The mean overlap time in which students from both classes are active (i.e., the time frame in which the mean number of entering students and the mean number of exiting students in the building are both positive) is illustrated in Figure 7(b).

Since more students are present, mean speeds stay below the levels that our pedestrians achieved in entering- or exiting-only simulations, as we show in Figure 7(a). These social-force interactions also increase the mean time that students take to reach their desired desk or building door, depending on their class. The travel-time distributions for entering and exiting students in Figure 7(c) both show longer tails than the corresponding distributions in Figures 5(c) and 6(c).

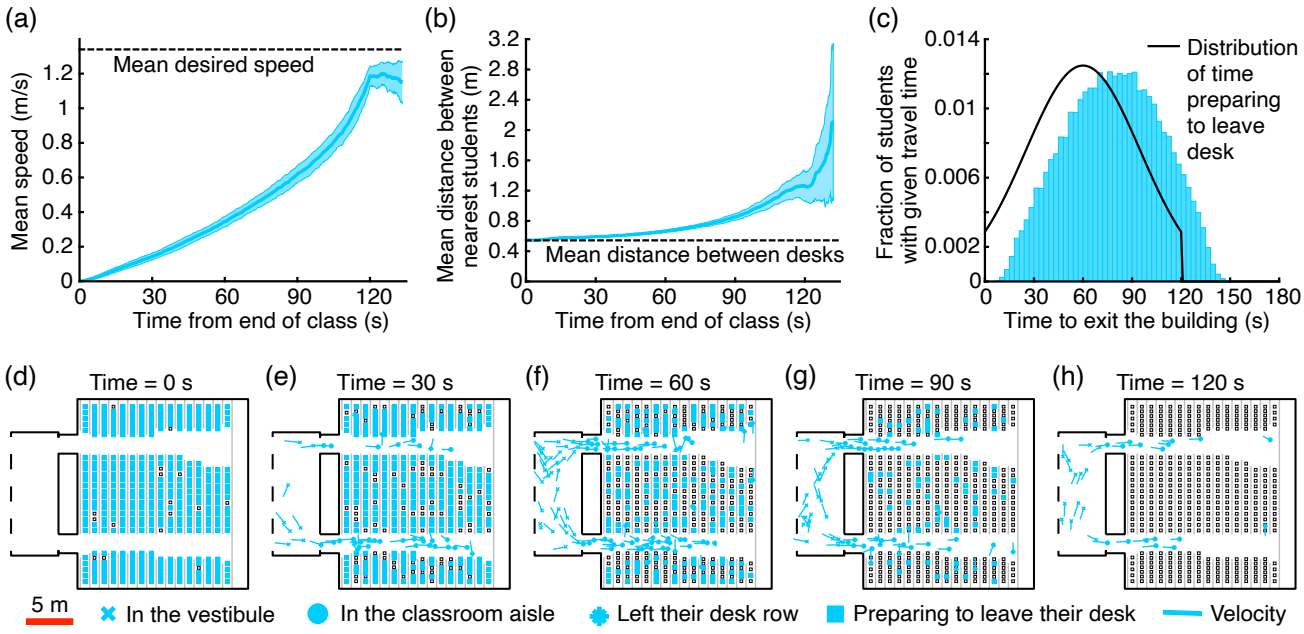

Figure 6. Exiting class of 400 students in our Rock Hall, with no entering class. Panels (a)–(c) present summary statistics across 100 simulations. (a) Students start with zero velocity at their desks and approach the mean desired speed in time. (b) As time passes, more students depart the building and the standard deviation in student–student distances grows. In panels (a)–(b), solid (shaded) lines indicate the average (standard deviation) over 100 simulations. (c) The distribution for the time that it takes students to exit the building after class ends has a similar shape as our distribution for the time (τ_i^{pre} for student i) that it takes students to gather their belongings and leave their desk. Histogram bin width is 3 s. (d)–(h) In this example simulation, blue squares denote students who are active but still gathering their belongings; these students can exert forces on others but do not feel forces themselves until $t \geq \tau_i^{\text{pre}}$; see Eq (2.5).

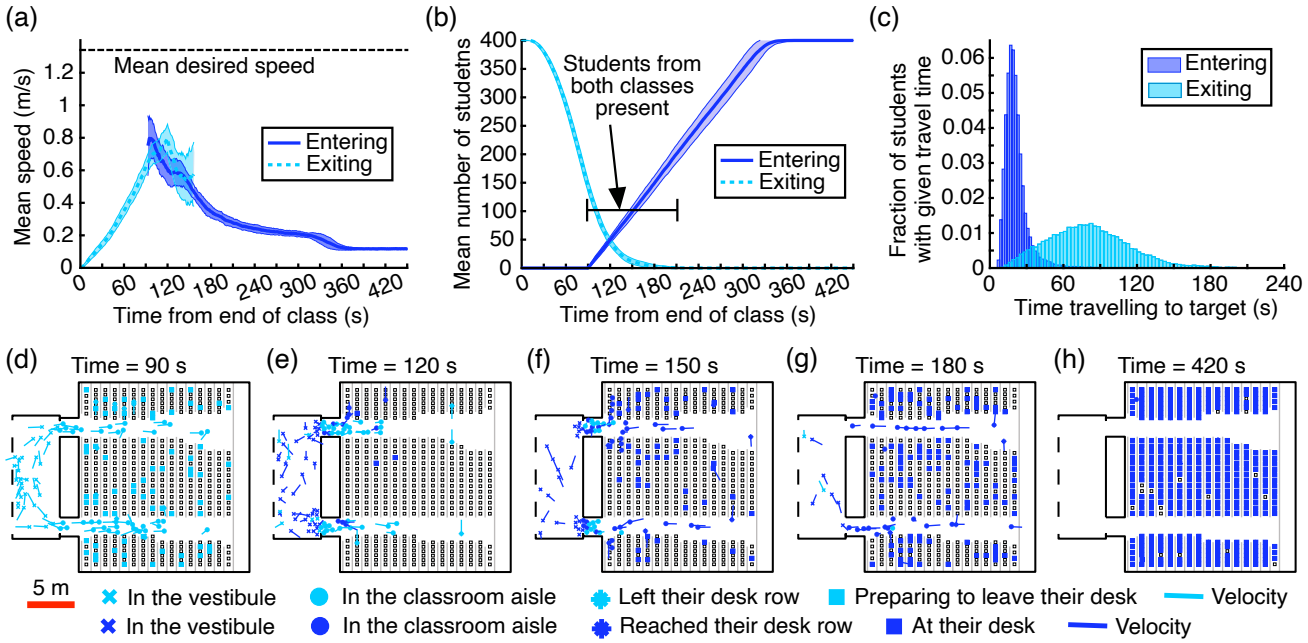

Figure 7. Consecutive classes of 400 students each in our Rock Hall, with one class exiting and the next class entering. Panels (a)–(b) present summary statistics across 100 simulations. (a) We indicate the mean desired speed (dashed line; see Eq (2.13)) and the mean speed for each class of students through time. We assume entering students do not begin arriving at the building doors until $t_{\text{sep}} = 90$ s after the end of the first class. (b) As time passes, fewer exiting students remain, and more entering students become active. In panels (a)–(b), solid (shaded) lines are the average (standard deviation) over 100 simulations. (c) The travel-time distributions have longer tails than in the entering-only (Figure 5(c)) and exiting-only (Figure 6(c)) simulations. Histogram bin widths are 2 s and 3 s for entering and exiting students, respectively. (d)–(h) In this example simulation, pedestrians interact with students from the other class mainly in the vestibule and at the classroom doors.

3.3. Effects of lecture-hall size on classroom-turnover times

Larger lecture halls require students to travel farther, so we expect the time that it takes a single class to enter or an isolated class to exit to scale with the size of the room. In cases of bidirectional movement, the possibility for congestion at the classroom doors adds further complexity. Here we investigate the impact of class size on the time that it takes for the prior class to exit and the new one to find their desks. We show how this classroom-turnover time also depends on the separation time between the end of the first class and when entering students start arriving.

To account for lecture halls of different sizes, we adapt our baseline Rock Hall domain to produce four more domains with 200, 328, 500, and 600 desks, respectively; see supplementary material for details. As we show in Supplementary Figure 2, all of our domains have the same vestibule, doors, and aisle widths, and they differ primarily in aisle length, rather than row length. This means that students spend more time moving down aisles as the room size increases, but the distance that they travel in tight rows of desks is about the same across our domains. In all of our simulations, we assume class sizes of 200 students in our 200-desk room, 300 in our 328-desk room, 400 in our baseline 416-desk room (Rock Hall), 500 in our 500-desk room, and 600 in our 600-desk room; we set $N^{\text{early}} = 0$ and $N^{\text{enter}} = N^{\text{exit}}$.

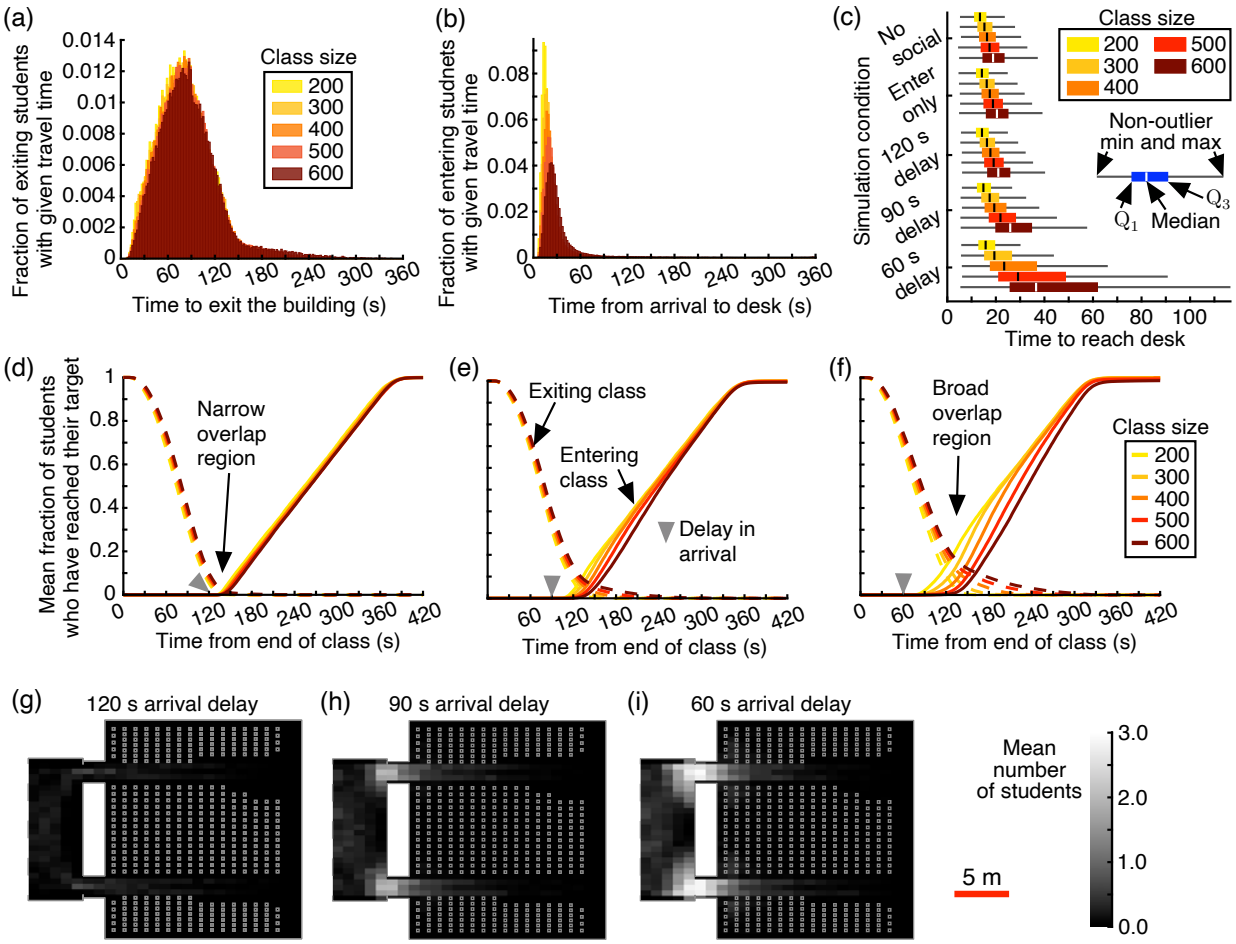

Figure 8. Consecutive classes for different lecture-hall sizes and separation times. We show summary statistics across 100 simulations for each class size and separation time. (a) The travel-time distributions for exiting students are positive-skewed. As class size increases, the long tails become more prominent. (b) The distributions for the time that it takes entering students to reach their desks (once they arrive at the building doors) also have long tails, and the mean travel time increases with class size. Panels (a)–(b) show different class sizes under a separation time of 90 s; histogram bin width is 3 s. (c) Medians, first and third quartiles (Q_1 and Q_3), and non-outlier minimum and maximum travel times for entering students. We observe a shift in the median travel time and growing positive skew as class size increases and separation time (or "delay" after the end of the class before the arrival of entering students) decreases. We define outlier travel times as values that fall below $Q_1 - 1.5(Q_3 - Q_1)$ or above $Q_3 + 1.5(Q_3 - Q_1)$; see supplementary material. "No social" refers to setting $B^{\text{rep}} = B^{\text{col}} = 0$ in Eq (2.12). We compute the results in panels (a)–(c) across all agents in 100 simulations. (d)–(f) We show the mean fraction of students in the exiting (dashed) and entering (solid) class who have reached their target under a separation time of 120 s, 90 s, and 60 s, respectively, across our 100 simulations. As the separation time decreases, there is a broader region of overlap with both classes present. (g)–(i) To highlight how congestion at the classroom doors increases with decreasing separation time, we show the mean mass (number of students in grid squares with area 1.5 m^2) at $t = 120$ s across 100 simulations of 400 entering and 400 exiting students in our Rock Hall. See supplementary material for more details and examples.

Figure 8(a) illustrates the effects of lecture-hall size on the time that it takes students in the first class to leave the building, assuming a separation time of 90 s between the end of the first class and the time that students in the next class begin arriving at the building doors. Similarly, Figure 8(b) shows the time that entering students spend travelling to their desks after they arrive to the building for rooms of different sizes. The mean travel time for exiting students changes relatively little—by about 15%—between the 200- and 600-person classrooms. In comparison, the mean travel time for entering students increases from about 16 s for the 200-person room to about 35 s for the 600-person room, more than doubling.

We now focus on entering students, since lecture-hall size has the largest impact on their travel times and classroom turnover depends on all of the students in the next class reaching their desks. Because the increase in mean travel time for entering students is partly due to the increasingly long tails in our distributions in Figure 8(b), it is also useful to consider median travel times in Figure 8(c). We find a similar dynamic: as class size increases from 200 to 600 students for a separation time of 90 s, the median time that it takes entering students to reach their desks grows from about 15 s to about 26 s.

To tease out whether increased student interactions are responsible for the additional time that entering students spend travelling in Figure 8(b) or if this is simply due to an increase in lecture-hall size, we simulate our model with no social forces. This means $\mathbf{f}^{\text{col}} = \mathbf{f}^{\text{rep}} = 0$ in Eq (2.5). Since each pedestrian in our model acts independently when there are no social forces, this is equivalent to considering only one student moving in the lecture hall. As we show in Figure 8(c), the median time that it takes entering students to reach their desks differs by only about 5 s between the 200- and 600-person classes, under the case of no social forces.

If we instead include social forces but assume that there is no exiting class, the median travel time for entering students increases by about 6 s between the 200- and 600-person classes. In comparison, there is a difference of about 11 s between the median travel times of entering students for 200- and 600-person classes when an exiting class is present (under a separation time of 90 s). We thus conclude that interactions between students in different classes—rather than simply an increase in the physical distance that students need to travel—are responsible for extending classroom-turnover times as lecture-hall size increases.

These observations suggest that the impact of lecture-hall size on classroom-turnover times may grow as the separation time between the end of the first class and when students in the next class begin arriving decreases. To test this, we simulate 100 realizations of our model for different lecture-hall sizes under a separation time of 120 s and 60 s, respectively. As we show in Figure 8(c), the impact of lecture-hall size on the time that entering students spend travelling to their desk (after arriving) is most pronounced under a 60 s separation time. In contrast, a separation time of 120 s leads to entering students having similar dynamics to the setting where there is no exiting class. Across our simulations, as lecture-hall size increases and separation time decreases, the median travel time for entering students increases and the long tail in our distributions becomes more prominent.

Our results in Figures 8(a)–(c) take a student-centered perspective, evaluating how long individuals spend travelling to their desks after they arrive at the building doors. To better understand the influence of separation time on overall classroom dynamics, we next consider the mean fraction of exiting and entering students who have reached their final target (a door or desk) as a function of time from the end of class, across 100 simulations for each lecture-hall size and separation time. As we show in Figures 8(d)–(f), the mean fraction of exiting students still in the building decays from one to zero in

time, and the mean fraction of entering students who are not yet at their desk, initially zero until the separation time has passed, grows as students arrive at the building doors and later reach their desks.

For the 120 s separation time in Figure 8(d), nearly all of the exiting students have left the building before entering students begin arriving. This can also be seen in Figure 8(g), which provides a heat map of the number of students in the building at $t = 120$ s. In comparison, a separation time of 90 s leads to a longer time interval in which both exiting and entering students are active. As we show in Figure 8(h), this creates congestion near the classroom doors. Finally, a separation time of 60 s in Figure 8(f) produces an even longer overlap region and heavy congestion (Figure 8(i)) at classroom doors.

Taken together, Figures 8(a)–(f) highlight that separation times have an opposite effect on the overall classroom dynamics than they do on the experiences of many individual students. As likely intended when scheduling classes, we find that a reduction in the time between classes generally leads to faster overall classroom-turnover times, amongst the separation times that we consider: Figures 8(d)–(f) show that the time that it takes from the end of the first class for 90% of the next class, on average, to have reached their desks is shorter for smaller separation times in our model. On the other hand, most entering students travel for a longer time to reach their desks as the separation time decreases. Our results therefore suggest that shorter separation times may increase frustration for these students, who arrive closer to the end of the first class and must wait in the vestibule due to congestion before they can enter the classroom.

4. Conclusions

Motivated by large lecture halls at colleges in the United States [72, 73, 81], we developed an off-lattice model for the movement of pedestrians in academic spaces. With a basis in the well-studied social-force approach [19, 49], which allows for the extensions necessary for our application, our model allows students in the entering class to arrive at building doors, move through a vestibule, and travel down classroom aisles to reach the row of their desk. Similarly, we modeled students in the exiting class as agents who leave their desks at random times after class ends and move toward building doors. We investigated classroom dynamics—with a focus on classroom-turnover times and the travel times of individual students—under different class settings (namely entering only, exiting only, or bidirectional), lecture-hall sizes, and separation times between classes.

Simulating our model without social forces showed that interactions between students play a critical role in classroom-turnover times. The separation time between the end of class and when students in the next class begin arriving determines how much exiting and entering students interact, and shorter separation times increase congestion at classroom doors. We found that the impact of the separation time between classes on student travel times is more pronounced in larger lecture halls. Interestingly, we also observed a discrepancy between the effect that separation time has on the travel time of individuals and on the time that it takes to empty and fill a classroom. While the median travel time for entering students decreased with increasing separation time, the time required to fill 90% of the class increased with increasing separation time, particularly in large lecture halls. This suggests that it is important to balance different perspectives when evaluating how the size of a lecture hall will influence student dynamics.

There are many directions for future work and points of improvement to address limitations of our model. For example, it is worth noting that the differences in student travel times for different room sizes seem relatively small—on the order of seconds—in Figure 8. Indeed, while in agreement with prior

studies of free, unhindered pedestrian movement [75], the speed that agents move in our model may be too high for a classroom environment. On the other hand, from an individual pedestrian's perspective, needing to wait an additional 16 s to enter a 200- versus a 600-person room may be tangible and frustrating. Future work could adjust our parameters to match data specific to lecture halls or theaters, and investigate how students perceive different waiting times [20]. It is also important to consider a broader range of pedestrian movement, including students travelling with wheelchairs or crutches, as well as classroom features such as changes in elevation (e.g., inclines or stairs) and other obstacles. We expect that some of these features may be more challenging to incorporate into the framework of social-force models.

One of the main limitations of our work is that our study focused fully on simulated dynamics. Designing experiments to track student volunteers moving in large lecture halls, including Rock Hall, is an especially important area for future research. Figure 8 shows that the time that it takes classrooms to fully turn over—roughly 5 minutes—in our simulations fits into the common separation time of about 10 minutes between consecutive classes in many universities; while this suggests that our model parameters may be in the right ballpark, future empirical studies with student volunteers will provide a valuable place for further model validation and testing. As empirical data becomes available, our modeling approach could be adapted and extended to help address questions about how large lecture halls affect the dynamics of student movement and class scheduling across a campus. For example, what is the limiting lecture-hall size at which universities need to increase the separation time between consecutive classes? By extending our model to include travel times between buildings, can one provide insight into class scheduling as universities build or adapt new lecture halls? To help support future modeling studies of student dynamics in large lecture halls, all of our code is available on GitLab [74].

In terms of additional limitations and future work, it is also important to better understand the role of modeling choices in our results. In particular, it will be interesting to compare alternative choices in model structure and implementation. For example, Chraibi et al. [82] have studied how directing pedestrians to target destinations according to different strategies affects movement. As we discuss in the supplementary material, we specified that students move toward the midpoint of classroom doors with some stochastic variation; future work could test how sensitive our results are to this simplification, particularly because we see higher congestion near doors. In a related direction, motivated by [83], one could implement alternative methods for assigning desired speeds.

Several studies (e.g., [84–86]) have compared multiple models of pedestrian dynamics alongside one another, particularly in the case of bidirectional movement and lane formation. It would be especially interesting to determine how alternative models affect the dynamics that we see near classroom doors and to quantify whether or not lane formation is present in our bidirectional simulations. In order to better understand if our results are model-dependent, implementing alternative models in our classroom domains is an important direction for future research. For example, the social-force approach can be adapted to incorporate features such as an effective angle of sight [1, 49] (to model pedestrians in front of a student having a larger impact on their movement than individuals behind them), or attractive forces between students in the same class [49] (which may lead to the formation of pedestrian groups). It would also be interesting to consider approaches such as the centrifugal-force model, which modifies the repulsion between two pedestrians depending on if the person in front is slowing down [87], and related models [82]. To further test our results, one could implement cellular automaton approaches, as well as other models that incorporate anticipation into movement (e.g., [86]).

Our results on separation times suggest that individuals may shorten how long it takes to reach their desk by choosing to arrive at the building doors later, particularly for large lecture halls. In contrast, from a collective perspective, arriving later prolongs the time that it takes to fill the classroom. In the future, it may be interesting to incorporate game-theoretic decision making into our model. Using our modeling setup, one could test whether different arrival choices create a dilemma in which the interests of individuals (i.e., minimizing their social interactions and travel times) conflict with the collective interest of emptying and filling the lecture hall in an efficient manner. Similar questions of strategic arrival times have been explored in many contexts, including queuing systems [88, 89], congestion and congestion pricing in traffic [90, 91], and start times for meetings [92].

More generally, our model does not include dynamic changes in the rules governing pedestrian behavior, and we assign each student their desk and building door at the start of a simulation. Future work could include allowing students to actively select their desks and doors in response to the current conditions in the lecture hall. For example, students could attempt to minimize the number of people that they must pass in narrow rows to reach their desk, or they could seek to optimize their preference to be near the front or the back of the class. It would also be interesting to extend our study to allow students to moderate their speeds based on perceived justness [20] or urgency. While our focus has been on understanding the role of lecture-hall size in routine settings, our modeling setup and code [74] could be adapted to investigate other conditions, including evacuation dynamics, lecture-hall design, or—related to the Covid-19 pandemic [93]—classroom dynamics under social distancing [10].

Acknowledgments

M.-V.C. has been supported by The Ohio State University President's Postdoctoral Scholars Program and by the Mathematical Biosciences Institute (MBI) at The Ohio State University and the National Science Foundation (NSF) through grant no. DMS-1440386. D.B.C. has been supported by the NSF through grant no. DMS-1514606, by the Army Research Office through grant no. W911NF-18-1-032x5, and by the Simons Foundation through the Math + X grant awarded to University of Pennsylvania. A.V. has been supported by the NSF through grant nos. DMS-1440386 and DMS-1764421, by the Simons Foundation/SFARI under grant no. 597491-RWC, and by the MBI. This collaboration is based upon work supported by the Mathematics Research Communities of the American Mathematical Society (AMS), under NSF grant no. DMS-1641020. Our project was initiated during the 2018 MRC on Agent-based Modeling in Biological and Social Systems. We are also grateful to the AMS MRC program for supporting a follow-up collaboration visit to the Mathematical Biosciences Institute. This collaboration was also supported by the NSF under grant no. DMS-1929284 through a visit to the Institute for Computational and Experimental Research in Mathematics in Providence, RI, during the "Mathematical Models of Pedestrian Movement in Large Lecture Halls" Collaborate@ICERM program. We thank Danielle Ciesielski and Andrew Bernoff for helpful discussions at the MRC workshop, and we also thank Chad Topaz for connecting AV and KB.

Conflict of interest

The authors declare there is no conflict of interest.

References

1. D. Helbing, L. Buzna, A. Johansson, T. Werner, Self-organized pedestrian crowd dynamics: Experiments, simulations, and design solutions, *Transp. Sci.*, **39** (2005), 1–24. https://doi.org/10.1287/trsc.1040.0108
2. N. Bellomo, D. Clarke, L. Gibelli, P. Townsend, B. J. Vreugdenhil, Human behaviours in evacuation crowd dynamics: From modelling to "big data" toward crisis management, *Phys. Life Rev.*, **18** (2016), 1–21. https://doi.org/10.1016/j.plrev.2016.05.014
3. A. Schadschneider, M. Chraibi, A. Seyfried, A. Tordeux, J. Zhang, Pedestrian dynamics: From empirical results to modeling, in *Modeling and Simulation in Science, Engineering and Technology*, Springer-Verlag, New York, 2018, 63–102. https://doi.org/10.1007/978-3-030-05129-7_4
4. D. C. Duives, W. Daamen, S. P. Hoogendoorn, State-of-the-art crowd motion simulation models, *Transp. Res. C: Emerg. Technol.*, **37** (2013), 193–209. https://doi.org/10.1016/j.trc.2013.02.005
5. B. Zhan, D. N. Monekosso, P. Remagnino, S. A. Velastin, L.-Q. Xu, Crowd analysis: a survey, *Mach. Vis. Appl.*, **19** (2008), 345–357. https://doi.org/10.1007/s00138-008-0132-4
6. E. Cristiani, B. Piccoli, A. Tosin, *Multiscale Modeling of Pedestrian Dynamics*, MS&A, Springer-Verlag, New York, 2014. https://doi.org/10.1007/978-3-319-06620-2
7. B. D. Hankin, R. A. Wright, Passenger flow in subways, *J. Oper. Res. Soc.*, **9** (1958), 81–88. https://doi.org/10.2307/3006732
8. A. A. Bartlett, The Frank C. Walz lecture halls: A new concept in the design of lecture auditoria, *Am. J. Phys.*, **41** (1973), 1233–1240. https://doi.org/10.1119/1.1987535
9. V. Romero, W. D. Stone, J. D. Ford, COVID-19 indoor exposure levels: An analysis of foot traffic scenarios within an academic building, *Transp. Res. Interdiscip. Perspect.*, **7** (2020), 100185. https://doi.org/10.1016/j.trip.2020.100185
10. S. Sajjadi, A. Hashemi, F. Ghanbarnejad, Social distancing in pedestrian dynamics and its effect on disease spreading, *Phys. Rev. E*, **104** (2021), 014313. https://doi.org/10.1103/PhysRevE.104.014313
11. M. Xu, X. Xie, P. Lv, J. Niu, H. Wang, C. Li, et al., Crowd behavior simulation with emotional contagion in unexpected multihazard situations, *IEEE Trans. Syst. Man Cybern.: Syst.*, **51** (2021), 1567–1581. https://doi.org/10.1109/TSMC.2019.2899047
12. D. Helbing, I. Farkas, T. Vicsek, Simulating dynamical features of escape panic, *Nature*, **407** (2000), 487–490. https://doi.org/10.1038/35035023
13. M. Haghani, M. Sarvi, Simulating dynamics of adaptive exit-choice changing in crowd evacuations: Model implementation and behavioural interpretations, *Transp. Res. Part C Emerg. Technol.*, **103** (2019), 56–82.
14. H. R. L. Lee, A. Bhatia, J. Brynjarsdóttir, N. Abaid, A. Barbaro, S. Butail, Speed modulated social influence in evacuating pedestrian crowds, *Collective Dyn.*, **5** (2020), 1–24. https://doi.org/10.17815/CD.2020.25
15. Z. Li, W. Xu, Pedestrian evacuation within limited-space buildings based on different exit design schemes, *Saf. Sci.*, **124** (2020), 104575.

16. E. Porter, S. H. Hamdar, W. Daamen, Pedestrian dynamics at transit stations: an integrated pedestrian flow modeling approach, *Transp. A: Transp. Sci.*, **14** (2018), 468–483. https://doi.org/10.1080/23249935.2017.1378280

17. S. P. Hoogendoorn, P. H. L. Bovy, Pedestrian route-choice and activity scheduling theory and models, *Transp. Res. B: Methodol.*, **38** (2004), 169–190. https://doi.org/10.1016/S0191-2615(03)00007-9

18. N. W. F. Bode, E. Ronchi, Statistical model fitting and model selection in pedestrian dynamics research, *Collective Dyn.*, **4** (2019), 1–32. https://doi.org/10.17815/CD.2019.20

19. D. Helbing, A. Johansson, *Pedestrian, Crowd and Evacuation Dynamics*, Springer, New York, 2009, 6476–6495. https://doi.org/10.1007/978-0-387-30440-3_382

20. A. Sieben, J. Schumann, A. Seyfried, Collective phenomena in crowds–Where pedestrian dynamics need social psychology, *PLOS ONE*, **12** (2017), e0177328. https://doi.org/10.1371/journal.pone.0177328

21. M. Davidich, F. Geiss, H. G. Mayer, A. Pfaffinger, C. Royer, Waiting zones for realistic modelling of pedestrian dynamics: A case study using two major German railway stations as examples, *Transp. Res. C: Emerg. Technol.*, **37** (2013), 210–222. https://doi.org/10.1016/j.trc.2013.02.016

22. D. Nilsson, A. Johansson, Social influence during the initial phase of a fire evacuation–Analysis of evacuation experiments in a cinema theatre, *Fire Saf. J.*, **44** (2009), 71–79. https://doi.org/10.1016/j.firesaf.2008.03.008

23. M. Moussaïd, E. G. Guillot, M. Moreau, J. Fehrenbach, O. Chabiron, S. Lemercier, et al., Traffic instabilities in self-organized pedestrian crowds, *PLOS Comput. Biol.*, **8** (2012), e1002442. https://doi.org/10.1371/journal.pcbi.1002442

24. S. P. Hoogendoorn, W. Daamen, Pedestrian behavior at bottlenecks, *Transp. Sci.*, **39** (2005), 147–159. http://www.jstor.org/stable/25769239

25. A. Seyfried, O. Passon, B. Steffen, M. Boltes, T. Rupprecht, W. Klingsch, New insights into pedestrian flow through bottlenecks, *Transp. Sci.*, **43** (2009), 395–406. http://www.jstor.org/stable/25769460

26. Y. Feng, D. Duives, W. Daamen, S. Hoogendoorn, Data collection methods for studying pedestrian behaviour: A systematic review, *Build. Environ.*, **187** (2021), 107329. https://doi.org/10.1016/j.buildenv.2020.107329

27. D. Helbing, Traffic and related self-driven many-particle systems, *Rev. Mod. Phys.*, **73** (2001), 1067–1141. https://link.aps.org/doi/10.1103/RevModPhys.73.1067

28. J. A. Carrillo, S. Martin, M.-T. Wolfram, An improved version of the Hughes model for pedestrian flow, *Math. Models Methods Appl. Sci.*, **26** (2016), 671–697. https://doi.org/10.1142/S0218202516500147

29. R. L. Hughes, A continuum theory for the flow of pedestrians, *Transp. Res. B: Methodol.*, **36** (2002), 507–535. https://doi.org/10.1016/S0191-2615(01)00015-7

30. R. L. Hughes, The flow of human crowds, *Annu. Rev. Fluid Mech.*, **35** (2003), 169–182. https://doi.org/10.1146/annurev.fluid.35.101101.161136

31. R. M. Colombo, M. Garavello, M. Lécureux-Mercier, A class of nonlocal models for pedestrian traffic, *Math. Models Methods Appl. Sci.*, **22** (2012), 1150023. https://doi.org/10.1142/S0218202511500230
32. A. L. Bertozzi, J. Rosado, M. B. Short, L. Wang, Contagion shocks in one dimension, *J. Stat. Phys.*, **158** (2015), 647–664. https://doi.org/10.1007/s10955-014-1019-6
33. R. Bürger, P. Goatin, D. Inzunza, L. M. Villada, A non-local pedestrian flow model accounting for anisotropic interactions and domain boundaries, *Math. Biosci. Eng.*, **17** (2020), 5883–5906. https://doi.org/10.3934/mbe.2020314 .
34. N. Bellomo, A. Bellouquid, D. Knopoff, From the microscale to collective crowd dynamics, *Multiscale Model. Simul.*, **11** (2013), 943–963. https://doi.org/10.1137/130904569
35. D. Kim, A. Quaini, Coupling kinetic theory approaches for pedestrian dynamics and disease contagion in a confined environment, *Math. Models Methods Appl. Sci.*, **30** (2020), 1893–1915. https://doi.org/10.1142/S0218202520400126
36. A. Festa, A. Tosin, M.-T. Wolfram, Kinetic description of collision avoidance in pedestrian crowds by sidestepping, *Kinet. Relat. Models*, **11** (2018), 491. https://doi.org/10.3934/krm.2018022
37. P. Degond, C. Appert-Rolland, J. Pettré, G. Theraulaz, Vision-based macroscopic pedestrian models, *Kinet. Relat. Models*, **6** (2013), 803–839. https://doi.org/10.3934/krm.2013.6.809
38. L. F. Henderson, The statistics of crowd fluids, *Nature*, **229** (1971), 381–383. https://doi.org/10.1038/229381a0
39. C. Burstedde, K. Klauck, A. Schadschneider, J. Zittartz, Simulation of pedestrian dynamics using a two-dimensional cellular automaton, *Physica A*, **295** (2001), 507–525. https://doi.org/10.1016/S0378-4371(01)00141-8
40. A. Varas, M. Cornejo, D. Mainemer, B. Toledo, J. Rogan, V. Muñoz, et al., Cellular automaton model for evacuation process with obstacles, *Physica A*, **382** (2007), 631–642. https://doi.org/10.1016/j.ssci.2010.09.006
41. J. Hu, L. You, H. Zhang, J. Wei, Y. Guo, Study on queueing behavior in pedestrian evacuation by extended cellular automata model, *Physica A*, **489** (2018), 112–127. https://doi.org/10.1016/j.physa.2017.07.004
42. A. Kirchner, A. Schadschneider, Simulation of evacuation processes using a bionics-inspired cellular automaton model for pedestrian dynamics, *Physica A*, **312** (2002), 260–276. https://doi.org/10.1016/S0378-4371(02)00857-9
43. V. J. Blue, J. L. Adler, Cellular automata microsimulation for modeling bi-directional pedestrian walkways, *Transp. Res. B: Methodol.*, **35** (2001), 293–312. https://doi.org/10.1016/S0191-2615(99)00052-1
44. Q. F. Gao, Y. Z. Tao, Y. F. Wei, C. Wu, L. Y. Dong, Simulation-based optimization of inner layout of a theater considering the effect of pedestrians, *Chin. Phys. B*, **29** (2020), https://doi.org/10.1088/1674-1056/ab6c44
45. A. Kirchner, H. Klüpfel, K. Nishinari, A. Schadschneider, M. Schreckenberg, Simulation of competitive egress behavior: Comparison with aircraft evacuation data, *Physica A*, **324** (2003), 689–697. https://doi.org/10.1016/S0378-4371(03)00076-1

46. D. Helbing, M. Isobe, T. Nagatani, K. Takimoto, Lattice gas simulation of experimentally studied evacuation dynamics, *Phys. Rev. E*, **67** (2003), 067101. https://doi.org/10.1103/PhysRevE.67.067101

47. Y. Tajima, T. Nagatani, Scaling behavior of crowd flow outside a hall, *Physica A*, **292** (2001), 545–554. https://doi.org/10.1016/S0378-4371(00)00630-0

48. H. Kuang, X. Li, T. Song, S. Dai, Analysis of pedestrian dynamics in counter flow via an extended lattice gas model, *Phys. Rev. E*, **78** (2008), 066117. https://doi.org/10.1103/PhysRevE.78.066117

49. D. Helbing, P. Molnár, Social force model for pedestrian dynamics, *Phys. Rev. E*, **51** (1995), 4282. https://doi.org/10.1103/physreve.51.4282

50. F. Zanlungo, T. Ikeda, T. Kanda, Social force model with explicit collision prediction, *EPL*, **93** (2011), 68005. https://doi.org/10.1209/0295-5075/93/68005

51. M. Li, Y. Zhao, L. He, W. Chen, X. Xu, The parameter calibration and optimization of social force model for the real-life 2013 Ya'an earthquake evacuation in China, *Saf. Sci.*, **79** (2015), 243–253. https://doi.org/10.1016/j.ssci.2015.06.018

52. S. Seer, C. Rudloff, T. Matyus, N. Brändle, Validating social force based models with comprehensive real world motion data, *Transp. Res. Proc.*, **2** (2014), 724–732. https://doi.org/10.1016/j.trpro.2014.09.080

53. A. Johansson, D. Helbing, P. K. Shukla, Specification of the social force pedestrian model by evolutionary adjustment to video tracking data, *Adv. Complex Syst.*, **10** (2007), 271–288. https://doi.org/10.1142/S0219525907001355

54. M. Ko, T. Kim, K. Sohn, Calibrating a social-force-based pedestrian walking model based on maximum likelihood estimation, *Transportation*, **40** (2013), 91–107. https://doi.org/10.1007/s11116-012-9411-z

55. A. Kneidl, D. Hartmann, A. Borrmann, A hybrid multi-scale approach for simulation of pedestrian dynamics, *Transp. Res. C: Emerg. Technol.*, **37** (2013), 223–237. https://doi.org/10.1016/j.trc.2013.03.005

56. C. Delcea, L. A. Cotfas, Increasing awareness in classroom evacuation situations using agent-based modeling, *Physica A*, **523** (2019), 1400–1418. https://doi.org/10.1016/j.physa.2019.04.137

57. R. Liu, D. Jiang, L. Shi, Agent-based simulation of alternative classroom evacuation scenarios, *Front. Archit. Res.*, **5** (2016), 111–125. https://doi.org/10.1016/j.foar.2015.12.002

58. A. Lachapelle, M. T. Wolfram, On a mean field game approach modeling congestion and aversion in pedestrian crowds, *Transp. Res. B: Methodol.*, **45** (2011), 1572–1589. https://doi.org/10.1016/j.trb.2011.07.011

59. C. Dogbé, Modeling crowd dynamics by the mean-field limit approach, *Math. Comput. Model.*, **52** (2010), 1506–1520. https://doi.org/10.1016/j.mcm.2010.06.012

60. X. Zheng, Y. Cheng, Modeling cooperative and competitive behaviors in emergency evacuation: A game-theoretical approach, *Comput. Math. Appl.*, **62** (2011), 4627–4634. https://doi.org/10.1016/j.camwa.2011.10.048

61. M. Burger, M. Di Francesco, P. A. Markowich, M.-T. Wolfram, On a mean field game optimal control approach modeling fast exit scenarios in human crowds, in *52nd IEEE Conference on Decision and Control*, 2013, 3128–3133. https://doi.org/10.1109/CDC.2013.6760360

62. E. Cartee, A. Vladimirsky, Anisotropic challenges in pedestrian flow modeling, *Commun. Math. Sci.*, **16** (2018), 1067–1093. https://dx.doi.org/10.4310/CMS.2018.v16.n4.a7

63. Y. Achdou, J. M. Lasry, Mean field games for modeling crowd motion, in *Contributions to Partial Differential Equations and Applications*, Springer, Cham, 2019, 17–42. https://doi.org/10.1007/978-3-319-78325-3_4

64. R. Bailo, J. A. Carrillo, P. Degond, *Pedestrian Models Based on Rational Behaviour*, 259–292, Springer, Cham, 2018. https://doi.org/10.1007/978-3-030-05129-7_9

65. L. Fu, J. Luo, M. Deng, L. Kong, H. Kuang, Simulation of evacuation processes in a large classroom using an improved cellular automaton model for pedestrian dynamics, *Procedia Eng.*, **31** (2012), 1066–1071. https://doi.org/10.1016/j.proeng.2012.01.1143

66. J. Zhang, W. Song, X. Xu, Experiment and multi-grid modeling of evacuation from a classroom, *Physica A*, **387** (2008), 5901–5909. https://doi.org/10.1016/j.physa.2008.06.030

67. K. Takimoto, T. Nagatani, Spatio-temporal distribution of escape time in evacuation process, *Physica A*, **320** (2003), 611–621. https://doi.org/10.1016/S0378-4371(02)01540-6

68. A. Garcimartín, I. Zuriguel, J. M. Pastor, C. Martín-Gómez, D. R. Parisi, Experimental evidence of the "faster is slower" effect, *Transp. Res. Proc.*, **2** (2014), 760–767. https://doi.org/10.1016/j.trpro.2014.09.085

69. M. Moussaïd, D. Helbing, G. Theraulaz, How simple rules determine pedestrian behavior and crowd disasters, *Proc. Natl. Acad. Sci. USA*, **108** (2011), 6884–6888. https://doi.org/10.1073/pnas.1016507108

70. J. Zhang, W. Klingsch, A. Schadschneider, A. Seyfried, Ordering in bidirectional pedestrian flows and its influence on the fundamental diagram, *J. Stat. Mech. Theory Exp.*, **2012** (2012), P02002. https://doi.org/10.1088/1742-5468/2012/02/P02002

71. Dateline Staff, New lecture hall on the (California Ave.) block, 2019, Last accessed: 27-01-2022. Available from: https://www.ucdavis.edu/news/new-lecture-hall-block

72. UC Davis Office of the University Registrar, General Assignment Classroom Guide: 194 Rock Hall, Last accessed: 27-01-2022. Available from: https://registrar-apps.ucdavis.edu/rooms/room2.cfm?RoomType=GeneralAssignment&ID=1

73. I. Fink and Associates Inc, The Ohio State University Instructional Space Feasibility Study Final Report, 2009, Last accessed: 27-01-2022. Available from: https://registrar.osu.edu/scheduling/spacestudyfinalreport.pdf

74. J. Benson, M. Bessonov, K. Burke, S. Cassani, M. V. Ciocanel, D. B. Cooney, et al., Code associated with "How do classroom-turnover times depend on lecture-hall size?", 2022. Available from: https://gitlab.com/modeling-pedestrian-dynamics/lecture-hall-dynamics/-/tree/main/

75. N. Waldau, P. Gattermann, H. Knoflacher, M. Schreckenberg, *Pedestrian and evacuation dynamics 2005*, Springer, Berlin, 2007. https://doi.org/10.1007/978-3-540-47064-9

76. K. Alden, M. Read, J. Timmis, P. S. Andrews, H. Veiga-Fernandes, M. Coles, *Spartan*: A comprehensive tool for understanding uncertainty in simulations of biological systems, *PLOS Comput. Biol.*, **9** (2013), e1002916. https://doi.org/10.1371/journal.pcbi.1002916

77. J. Cosgrove, J. Butler, K. Alden, M. Read, V. Kumar, L. Cucurull-Sanchez, et al., Agent-based modeling in systems pharmacology, *CPT: Pharmacometrics Syst. Pharmacol.*, **4** (2015), 615–629. https://doi.org/10.1002/psp4.12018

78. M. Read, P. S. Andrews, J. Timmis, V. Kumar, Techniques for grounding agent-based simulations in the real domain: A case study in experimental autoimmune encephalomyelitis, *Math. Comput. Model. Dyn. Syst.*, **18** (2012), 67–86. ttps://doi.org/10.1080/13873954.2011.601419

79. A. Vargha, H. D. Delaney, A critique and improvement of the CL common language effect size statistics of McGraw and Wong, *J. Educ. Behav. Stat.*, **25** (2000), 101–132. https://doi.org/10.3102/10769986025002101

80. S. Cassani, S. D. Olson, A hybrid model of cartilage regeneration capturing the interactions between cellular dynamics and porosity, *Bull. Math. Biol.*, **82** (2020), 1–32. https://doi.org/10.1007/s11538-020-00695-1

81. CollegeData.com, 1st Financial Bank USA, 2022, Last accessed: 27-01-2022. Available from: https://waf.collegedata.com/college-search

82. M. Chraibi, M. Freialdenhoven, A. Schadschneider, A. Seyfried, Modeling the desired direction in a force-based model for pedestrian dynamics, in *Traffic and Granular Flow '11*, Springer, Berlin, 2013, 263–275. https://doi.org/10.1007/978-3-642-39669-4_25

83. L. Ma, B. Chen, L. Chen, X. Xu, S. Liu, X. Liu, Data driven analysis of the desired speed in ordinary differential equation based pedestrian simulation models, *Physica A*, **608** (2022), 128241. https://doi.org/10.1016/j.physa.2022.128241

84. F. Zanlungo, C. Feliciani, Z. Yücel, K. Nishinari, T. Kanda, Analysis and modelling of macroscopic and microscopic dynamics of a pedestrian cross-flow, preprint, arXiv:2112.12304.

85. D. Wolinski, S. J. Guy, A. H. Olivier, M. Lin, D. Manocha, J. Pettré, Parameter estimation and comparative evaluation of crowd simulations, *Comput. Graph Forum.*, **33** (2014), 303–312, https://doi.org/10.1111/cgf.12328 .

86. Q. Xu, M. Chraibi, A. Seyfried, Anticipation in a velocity-based model for pedestrian dynamics, *Transp. Res. Part C Emerg. Technol.*, **133** (2021), 103464. https://doi.org/10.1016/j.trc.2021.103464

87. W. J. Yu, R. Chen, L. Y. Dong, S. Q. Dai, Centrifugal force model for pedestrian dynamics, *Phys. Rev. E*, **72** (2005), 026112. https://doi.org/10.1103/PhysRevE.72.026112

88. A. Rapoport, W. E. Stein, J. E. Parco, D. A. Seale, Equilibrium play in single-server queues with endogenously determined arrival times, *J. Econ. Behav. Organ.*, **55** (2004), 67–91. https://doi.org/10.1016/j.jebo.2003.07.003

89. S. Juneja, N. Shimkin, The concert queueing game: strategic arrivals with waiting and tardiness costs, *Queueing Syst.*, **74** (2013), 369–402. https://doi.org/10.1007/s11134-012-9329-3

90. D. Levinson, Micro-foundations of congestion and pricing: A game theory perspective, *Transp. Res. A: Policy Pract.*, **39** (2005), 691–704. https://doi.org/10.1016/j.tra.2005.02.021

91. A. Ziegelmeyer, F. Koessler, K. B. My and L. Denant-Boèmont, Road traffic congestion and public information: An experimental investigation, *J. Transp. Econ. Policy*, **42** (2008), 43–82.

92. O. Guéant, J. M. Lasry, P. L. Lions, Mean field games and applications, in *Paris-Princeton Lectures on Mathematical Finance 2010*, Springer, Berlin, 2011, 205–266. https://doi.org/10.1007/978-3-642-14660-2_3

93. H. Harapan, N. Itoh, A. Yufika, W. Winardi, S. Keam, H. Te, et al., Coronavirus disease 2019 (COVID-19): A literature review, *J. Infect. Public Health*, **13** (2020), 667–673. https://doi.org/10.1016/j.jiph.2020.03.019

AIMS Press